*Desalination and Water Treatment*
www.deswater.com

doi: 10.5004/dwt.2022.28399

257 (2022) 64–75
May

# Analysis and optimization of operating conditions on ultrafiltration of landfill leachate using a response surface methodological approach

Mohamed Zait[a], Fatima Zahra Addar[a], Nawal Elfilali[a], Mustapha Tahaikt[a], Azzedine Elmidaoui[a], Mohamed Taky[a,b,*]

[a]*Laboratory of Advanced Materials and Process Engineering, Faculty of Sciences, Ibn Tofail University, BP 1246, Kenitra – Morocco, emails: Mohamed.taky@uit.ac.ma/takymohamed@gmail.com (M. Taky), mohamed.zait@uit.ac.ma (M. Zait), fatima.zahra@uit.ac.ma (F.Z. Addar) nawal.elfilali@uit.ac.ma (N. Elfilali), mustapha.tahaikt@uit.ac.ma (M. Tahaikt), elmidaoui@uit.ac.ma (A. Elmidaoui)*
[b]*International Water Research Institute, Mohammed VI Polytechnic University, Lot 660, Hay Moulay Rachid, Ben Guerir, 43150 – Morocco*

Received 16 December 2021; Accepted 14 March 2022

**ABSTRACT**

The term "leachate" or "landfill juice" refers to the water that has percolated through the waste and has become highly polluted. The pollution indicators total suspended solids (TSS), chemical oxygen demand (COD), biological oxygen demand and salinity of this effluent far exceed the discharge standards. In addition, the increasing requirements of the standards and the stabilization of leachates over time, new techniques have emerged to remedy this problem. Among the technologies used, we find reverse osmosis which has developed in many European countries. In Morocco, at the Oum Azza plant, leachates are treated by reverse osmosis because of their very high salinity. To avoid repeated fouling of the membranes, the pre-treatment must be efficient to meet the requirements of this process. This paper discusses the efficiency of ultrafiltration (UF) as a pretreatment of reverse osmosis in leachate treatment using three ceramic membranes. The response surface method (RS which is an analytical tool and an efficient approach to build predictive models and optimize the UF process was used. Influence of transmembrane pressure (TMP) and circulation velocity (CV) on the performance of three ceramic UF membranes of different pore sizes (UF20, UF50, UF100) for landfill leachate (LFL) treatment is studied. The response surface methodology based central composite design is applied to optimize the operational variables: TMP and CV. Quadratic models developed for the three responses permeate flux, COD and TSS indicate that rejection of COD and TSS obtained are respectively 85%, 66.8% for UF20, 76% and 62.6% for UF50 and finally 70.6% and 50.5% for UF100. Analysis of variance is used to study the variables and the interaction between them. A coefficient of determination found ($R^2 > 0.8$) for all three membranes shows a good correlation between experimental and predicted response values. In addition, response surface plots are drawn for spatial presentation with the regression equations. These results provide a new information on the effects of porosity and operating parameters on the performance of UFs membranes.

*Keywords:* Ultrafiltration; Response surface methodology; Central composite design; Optimization; Transmembrane pressure; Circulation velocity

* Corresponding author.

*Presented at the Second International Symposium on Nanomaterials and Membrane Science for Water, Energy and Environment (SNMS-2021), June 1–2, 2022, Tangier, Morocco*

## 1. Introduction

Despite the standard (ISO 14000 version 2000) stipulating a rational management of household waste landfills, leachates from household waste landfills can cause disturbances to aquatic, underground and surface ecosystems. For example, leachate from uncontrolled or poorly operated landfills can leach into the subsurface and contaminate groundwater. In fact, given the complex pollutant load of landfill leachate (LFL), it poses a real threat to the environment and human health. Due to the harmfulness of these effluents on the environment, a series of purification treatments is necessary before their release into the receiving environment or their reuse for internal purposes.

Considering the recent advances in membrane technologies, membrane processes, namely reverse osmosis (RO), nanofiltration (NF) and ultrafiltration (UF), have been used extensively in developed countries for LFL treatment [1,2]. Since the 1990s, membrane-based LFL treatment technologies have been used in landfills in some European countries (e.g., Germany) [3] and in North America due to its low production costs, high flexibility and high performance [4]. However, the fouling of the membranes, which is due to the organic pollution load of the leachate, causes frequent stops for washing and reduces the service life of the membranes used. To overcome this problem, a thorough pre-treatment is possible. Among the processes that can be used is UF, which is a promising method for the removal of organic matter in suspension.

RO and membrane bioreactor (MBR) methods have been applied to remove of heavy metals, inorganic, and organic compounds from LFL in conjunction with the conventional biological treatment and physicochemical methods [5,6]. The Seneca Meadows Landfill, which is the biggest active landfill site in New York State (USA), is a good example of a successful application of a membrane process for the treatment of LFL. According to Kaur et al. [7] RO allows to achieve a higher pollutant removal efficiency (>95%) and treat a large volume of LFL with a low capital cost investment.

The major drawback of LFL treatment by membrane processes is the production of concentrated wastewater (brine), which is a dark-colored solution containing refractory pollutants and high totally dissolved solids (TDS). Although the volume of the produced concentrates by membrane processes in LFL treatment represent only 13% to 50% of the initial LFL volume [8,9], it contains high levels of refractory organic pollutants such as aromatic compounds, endocrine disruptors, long chain hydrocarbons, halohydrocarbons, and inorganic salts. Moreover, the high concentration of saline compounds along with the presence of the above refractory pollutants greatly reduces the biodegradability of landfill leachate membrane concentrates (LLMCs) making it virtually untreatable by the biological treatment process. Therefore, conventional treatment methods (evaporation, recirculation, adsorption, membrane distillation, electrodialysis, coagulation, and oxidation) and advanced processes such as ozone-based processes, Fenton and persulfate-based oxidation processes, and electrochemical processes have been widely applied by many researchers for the treatment of LLMCs [10,11].

Talałaj et al. [12] combined MBR, activated sludge, a rotating biological contactor, and up-flow anaerobic sludge blanket treatments, followed by RO for the treatment of LFL. They removed 99%–99.5% of chemical oxygen demand (COD) and 99%–99.8% of ammoniacal nitrogen ($N–NH_4^+$) by coupling RO and activated sludge. Whereas, the combination of RO and rotating biological contactor allowed to reduce 99% of COD and $N–NH_4^+$. And finally, the combination of RO, activated sludge and rotating biological contactor allows removal of 98%–99.2% of chloride and 99%–99.7% of lead. Total suspended solids (TSS) are best removed up to 99%, by either a combination of RO with MBR, or RO with activated sludge.

Chiemchaisri et al. [13] treated LFL by a two-stage MBR, the abatement obtained are 99.6% for biological oxygen demand ($BOD_5$), 68% for COD, 89% for $NH_3$ and 86% for total nitrogen (TN).

In another study carried out by Liu et al. [14], with a configuration of two-stage anoxic/oxic combined MBR system for LFL, the abatement obtained reaches 80.60% for COD, 99.04% for $N–NH_4^+$ and 74.87% for TN.

Elfilali et al. [15] tested the combination of a MBR with RO to treat a highly loaded LFL with COD of 7,433 mg/L, $BOD_5$ of 1,250 mg/L and TSS of 387 mg/L. Removal rates of 95% were obtained for COD, $BOD_5$ and TSS. Although we have achieved these results, there are limitations of this combination, which is expressed as the biological and membrane processes (MBR) is that they do not completely remove salts, metals and organic molecules, in addition to rapid fouling of the UF membrane which influences the performance of the MBR. Moreover, the permeate obtained by the MBR process cannot be put directly into the RO, because of their high salinity. Also, the coupling of MBR/RO is limited by its operating cost which is high are estimated at 3.86 US $/m^3$.

Amaral et al. [16] combined MBR with NF processes for the treatment of LFL. This combination led to a great result in the elimination of COD, ammonia, color and toxicity close to 88%, 95%, 100% and 100%, respectively. Moreover, Li et al. [17] developed an integrated biological treatment process to treat LL which consist in a combination of an up-flow anaerobic sludge blanket (UASB), a continuous microfiltration (MF), a sequencing batch reactor (SBR) and RO technologies. The combined process allows to achieve removal of 99.5% of TN, 99.8% of COD and 99.8% of $BOD_5$.

The treatment of the Oum Azza LFL (Rabat, Morocco) is a combination of biological pretreatment, which consists of an aeration tank and an anoxic tank followed by a bag filter, and RO membrane treatment according to the diagram of Fig. 1. The frequent shutdowns for cleaning the fouled membranes due to the poor quality of the effluent after the pretreatment have pushed the drifters to study the feasibility of UF as a pretreatment upstream of the RO processes at the laboratory scale. In a previous work, three ultrafiltration membranes of different porosity (UF20 nm, UF50 nm and UF100 nm) were tested as pretreatment of the LFL of Oum Azza and removal rates of 85% for COD and 70.4% for TSS were obtained [18]. The obtained results also show a clear improvement of the effluent quality compared to the existing pretreatment and will allow to reduce the fouling of RO membranes and thus the frequencies of washing and stops.

Response surface methodology (RSM) is a simple and widely used tool for detecting and quantifying the influence of selected independent variables (factors) on the dependent variables (responses) and for process optimization [19]. For the purpose of the analysis, the experimental measurement must be organized using an appropriate experimental design (DOE) [20]. Factorial designs provide the opportunity to obtain more extensive and varied information about the system and very useful conclusions [21]. The RSM has been successfully used in studies on membrane processes, for the purpose of process optimization. Zolfaghari et al. [22] optimized the combination of a MBR equipped with UF and an electro-oxidation (EO) process using central composite design (CCD), in order to effectively treat highly contaminated LFLs. with the optimal conditions found, the COD, TOC (total organic carbon) and ammonium concentrations were reduced to 89.57 and 65 mg/L, respectively.

Many researchers have used RSM for process optimization. A study by Cojocaru and Zakrzewska-Trznadel [23] focused on the removal of $Cu^{2+}$ ions by UF using the RSM method to optimize hydrodynamic conditions. The results obtained a 99% $Cu^{2+}$ removal rate, where the optimal conditions found are $P$ = 0.19 bar, $Q_R$ = 54 L/h, $W$ = 41.33 Hz (2,480 rpm). Calatayud et al. [24] optimized the operating conditions (transmembrane pressure (TMP) and circulation velocity (CV) of two UF membranes (CARBOSEP M2 and TamiMSKT) using RSM, in order to treat a polyethylene glycol solute with a molecular weight of 35 kDa. They obtained the optimum conditions for the CARBOSEP M2 membrane as follows for the PTM is 0.38 MPa and a CV of 3 m/s. However, for the TamiMSKT membrane, the optimum conditions could not be determined due to the low precision of the regression model obtained for the cumulative permeation flux decline response variable. Darvishmotevalli et al. [25] optimized an electrochemical oxidation process for the treatment of saline wastewater using the RSM method, the optimal conditions found are pH 7.69, reaction time of 30.71 min, salt content of 30.94 g/L and voltage of 7.41 V, the removal rates of COD and TOC were 91.78% and 68.49%, respectively.

Any type of process used for the treatment of leachate always faces a lot of problems because of the complexity of the stabilized leachates effluents that are more than 10 years old, have a low $BOD_5$/COD ratio, their treatment by biological methods is difficult due to their low biodegradability. A study carried out by Bashir et al. [26,27] on the treatment of stabilized leachates, by aerobic biodegradation coupled with powdered activated carbon (PAC) was insufficient in particular to eliminate color and COD. But with the cationic resin alone they obtained 91.8% $NH_3$–N removal and the removal rates were insufficient for color at 68% and 38% for COD. Abuabdou et al. [28] tested the treatment of leachate by an anaerobic membrane bioreactor (AnMBR) at temperatures below 20°C and obtained a reduction in biomass growth, which translates into a sludge retention time (SRT) longer for stabilization. Many authors have confirmed that membrane process could be one of the best leachate treatment methods. However, the membranes are fouled easily when too many contaminants are present and in addition the membranes found on the market are not suitable for this type of effluent. Fouling can affect membrane permeability and separation efficiency, which are the two most important elements of the membrane separation system [26]. The objective of this work is to study and compare the performances of three UF ceramic membranes with different pore sizes, as pretreatment of RO. The influence of the TMP, the circulation velocity and the cut-off threshold of the membranes has been studied.

RSM is becoming more and more an indispensable tool for researchers because of its power in predicting, optimizing and studying the influence of different parameters of the studied systems. In order to model and optimize the LFL treatment process by the three tested membranes, DOE and RSM are used in this study. In addition, CCD coupled with RSM is chosen to simultaneously study the effects of TMP and CV on the three responses, namely permeate flux (PF), COD, and TSS. The optimal values of the operating parameters are obtained to maximize (PF), minimize the other two responses (COD and TSS). The experimental data are analyzed by fitting a second-order polynomial model, which is statistically validated by performing an analysis of variance (ANOVA). In addition, response surface plots are drawn for spatial presentation with the regression equations. These results provide new insights into the effects of porosity and operating parameters on the performance of UFs membranes.

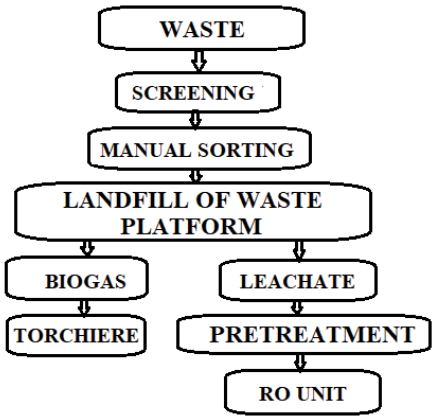


Fig. 1. Operating stages of the Oum Azza landfill plant.

## 2. Materials and methods

The LFL is periodically taken from the controlled dump of Oum Azza (110 ha) which is located in the commune of Oum Azza at 20 km from Rabat. This controlled Technical Landfill Center (CTC) was created in December 2007. The center receives significant tonnages ranging from 2,500 to 2,800 t/d of household waste from the three transfer centers: Rabat, Temara and Salé. The daily quantity of LFL produced in the landfill is 660 $m^3$/d, with an average age of 10 y.

Samples collected are transported to the laboratory to be analyzed and treated within hours following the collection.

Experiments are performed on a UF laboratory pilot supplied by the French company TIA (Technologies Industrielles Appliquées). It consists of a feeding tray with a capacity of 50 L and two pumps: one for circulation and

the other for filtration (Fig. 2). The tangential speed of recirculation is in the range 0.5–6 m/s. The TMP varies from 0 to 10 bar.

Table 1 gives the main characteristics of the membranes used. After UF tests, the membranes are cleaned with alkaline and acidic cleaning solutions according to the manufacturer's recommendations.

Permeate samples are collected and LFL parameters are determined analytically following standard methods:

Measurement COD (NF T90-101) is made according to AFNOR standards (1994). Determination of TSS (NF T90-105-2) is carried out according to the AFNOR standard (1997).

Retention $R(\%)$ is defined according to Eq. (1):

$$R(\%) = \frac{C_0 - C_p}{C_0} \times 100 \quad (1)$$

where $C_p$ and $C_0$ are permeate and initial concentrations respectively.

### 2.1. Modelling and statistics

For modeling and optimization of UF processes using three membranes, RSM which is based on CCD is applied, to understand the statistical significance of the variable parameters including: TMP ($X_1$) and CV ($X_2$). For the choice of the CCD design range is based on the respect of two criteria of optimality:

- *Orthogonality*: *criterion*: If the submatrix obtained by removing the first row and the first column of the matrix is diagonal, the criterion of near orthogonality is respected.
- *Isovariance by rotation criterion*: It is desired that the responses calculated with the model from the design of experiments have an identical prediction error for points located at the same distance from the center of the study domain. For the choice of condition of CCD design is based on the experiences of screening. These factors are varied at five different levels (–1.14, –1, 0, +1, +1.14), as shown in Table 2.

The process responses investigated for the model are FP, COD, and TSS. The sum of experimental design runs $N$, can be evaluated using Eq. (2).

$$N = 2^k + 2k + N_c \quad (2)$$

where $k$ is the number of input factors. The terms $2^k$, $2k$ and $N_c$ represent the factorial points, the axial points, and the center points, respectively.

## 3. Results and discussion

### 3.1. Characterization of the raw LFL

The main LFL analysis are presented in Table 3. The sampling campaign was achieved during January 2019.

Table 1
Characteristics of the membranes

| Characteristics | UF 1 | UF 2 | UF 3 |
|---|---|---|---|
| Pore size (nm) | 20 | 50 | 100 |
| Nature | Ceramic | Ceramic | Ceramic |
| Surface ($m^2$) | 0.35 | 0.35 | 0.24 |
| Maximum pressure (bar) | 10 | 10 | 10 |
| Maximum temperature (°C) | 100 | 100 | 100 |
| pH range | 3–11 | 3–11 | 3–11 |

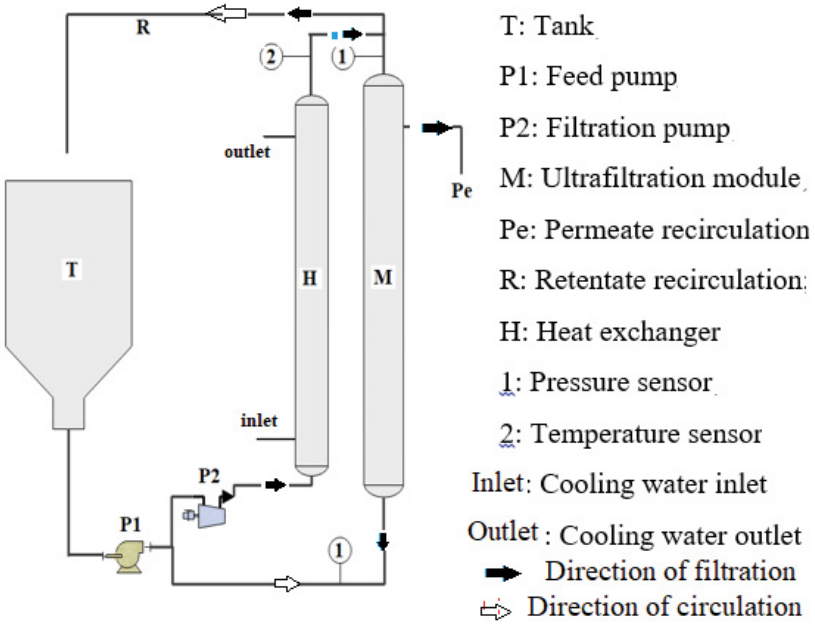


Fig. 2. Diagram of the UF pilot plant.

As shown in Table 3, all the pollution indicator contents exceed the discharge limit values [29].

These analyses show a strong organic pollution which results in high load of $BOD_5$, COD, TSS and a high electric conductivity. The average temperature of 18.6°C is fairly characteristic of the month during which the samples were taken and this recorded value is much lower than the value recommended for the (general limit value of discharge) [18].

### 3.2. Statistical analysis and modelling by RSM

The experimental data are collected after the completion of 13 experiments. The experimental results for all coded factors and actual response values for UF for the three membranes are presented in Table 4.

The performance of each UF is evaluated in terms of PF ($Y_1$), COD ($Y_2$) and TSS ($Y_3$) which are considered as responses. The following polynomial equation describes the predicted values of the responses $Y_1$, $Y_2$ and $Y_3$ as:

$$Y_1, Y_2 \text{ and } Y_3 = \beta_0 + \sum_{i=1}^{2}\beta_i X_i + \sum_{i=1}^{2}\sum_{j=1}^{2}\beta_{ij} X_i X_j + \sum_{i=1}^{2}\beta_{ii} X_i^2 + \xi \quad (3)$$

Table 2
Independent input variables range in terms of coded levels

| Factors | Coded level | | | | |
|---|---|---|---|---|---|
| | –1.414 | –1 | 0 | +1 | +1.414 |
| TMP (bar): (UF20, UF50 and UF100) | 2 | 3 | 5.55 | 8 | 9 |
| CV (m/s): (UF20, UF50 and UF100) | 0.77 | 1.5 | 3.25 | 5 | 5.72 |

Table 3
Physico-chemical and organic characterization of LFL and Moroccan discharge limit values

| Settings | Value | Domestic discharge limit values [24] |
|---|---|---|
| pH | 8.5 | 5.5–9.5 |
| Temperature (°C) | 18.6 | 30 |
| Electrical conductivity (mS/cm) | 30 | 2,700 |
| COD (mg/L) | 8,000 | 500 |
| $BOD_5$ (mg/L) | 4,120 | 100 |
| TSS (mg/L) | 4,500 | 100 |
| $NH_4^+$ (mg/L) | 150 | – |
| $HCO_3^-$ (mg/L) | 12,810 | – |
| $Cl^-$ (mg/L) | 3,650 | – |
| $NO_3^-$ (mg/L) | 4.1 | – |
| $PO_4^{3-}$ (mg/L) | 4.9 | – |
| $Ca^{2+}$ (mg/L) | 7.6 | – |
| $Mg^{2+}$ (mg/L) | 230 | – |
| $K^+$ (mg/L) | 6,000 | – |
| $Na^+$ (mg/L) | 4,800 | – |

where $Y_1$, $Y_2$, and $Y_3$ are the predicted responses, $\beta_0$ is the constant coefficient, $\beta_i$ is the linear coefficients, $\beta_{ij}$ is the interaction coefficients, $\beta_{ii}$ is the quadratic coefficients, and $X_i$ and $X_j$ are the coded values of the variables TMP and CV, $\varepsilon$ is the residual term (followed by the equation).

The experimental design and analysis of the experimental data are performed using the software (Design-Expert). Model fit and significance are determined by analysis of variance (ANOVA). The equation quality of the polynomial model is statistically estimated by the $R^2$ correlation coefficient. The more closely the coefficient of multiple determination $R^2$ is to 1, the better the fit of the module [30].

The significance and performance of the regression model is examined by ANOVA analysis of variance for LFL treatment by UF, the results are presented in Table 5. The *F*-values of all three models for all three membranes are satisfactory, implying that the model is significant at 95% confidence level. For the model term to be significant at this confidence level, the calculated probability must be ("Prob. > *F*" less than 0.05) for LFL treatment by UF20, UF50 and UF100. When they are greater than 0.5 and not significant, they indicate that the quad model is acceptable. The reliability of the model and the goodness of fit of the model values to the experimental data is demonstrated by the adjusted *R*-squared correlation coefficient (Adj.-$R^2$) which is greater than 0.8 for all the three membranes. Diagnostic plots such as predicted vs. actual values are used to judge the satisfaction of the model.

The regression equations for PF for UF20, UF50, and UF100 are given by Eqs. (4)–(6), respectively.

$$Y_1 = -7.53734 + 7.40141X_1 + 18.98205X_2 + 2.74402X_1X_2 - 0.612870X_1^2 - 3.07878X_2^2 \quad (4)$$

$$Y_1 = +62.27461 - 10.13227X_1 - 6.44442X_2 + 5.22624X_1X_2 + 0.932112X_1^2 + 0.204898X_2^2 \quad (5)$$

$$Y_1 = +223.28434 - 41.32132X_1 - 50.23234X_2 + 11.52886X_1X_2 + 3.38182X_1^2 + 4.80224X_2^2 \quad (6)$$

The regression equations for COD for UF20, UF50 and UF100 are given by Eqs. (7)–(9), respectively.

$$Y_2 = +5,945.61733 - 1,432.69007X_1 + 17.12658X_2 + 1.39942X_1X_2 - 0.734694X_1^2 + 103.54852X_2^2 \quad (7)$$

$$Y_2 = +6,533.21220 - 1,256.87573X_1 - 94.37316X_2 - 1.53936X_1X_2 - 84.35652X_1^2 + 14.22041X_2^2 \quad (8)$$

$$Y_2 = +4,841.51 - 814.46035X_1 - 154.0050X_2 - 6.2973X_1X_2 + 55.7994X_1^2 + 31.5260X_2^2 \quad (9)$$

The regression equations for TSS for UF20, UF50 and UF100 are given by Eqs. (10)–(12), respectively.

Table 4
CCD for the two independent variables

| Run | Coded variables values | | Responses values | | | | | | | | |
|---|---|---|---|---|---|---|---|---|---|---|---|
| | | | UF20 | | | UF50 | | | UF100 | | |
| | $X_1$ | $X_2$ | $Y_1$ | $Y_2$ | $Y_3$ | $Y_1$ | $Y_2$ | $Y_3$ | $Y_1$ | $Y_2$ | $Y_3$ |
| 1 | 0 | 0 | 93.33 | 1,206.4 | 1,365.3 | 110.24 | 2,027.2 | 1,759.95 | 193.54 | 2,461.6 | 2,291.85 |
| 2 | 0 | 0 | 93.33 | 1,206.4 | 1,365.3 | 110.24 | 2,027.2 | 1,759.95 | 193.54 | 2,461.6 | 2,291.85 |
| 3 | –1 | 1 | 70.4 | 2,392 | 2,740.95 | 88.91 | 3,347.2 | 2,875.95 | 154.78 | 3,515.2 | 2,917.35 |
| 4 | 1 | –1 | 73.46 | 1,240 | 1,287 | 88 | 1,820 | 1,694.7 | 176.23 | 2,228 | 2,038.5 |
| 5 | 0 | 0 | 93.33 | 1,206.4 | 1,365.3 | 110.24 | 2,027.2 | 1,759.95 | 193.54 | 2,461.6 | 2,291.85 |
| 6 | –1.414 | 0 | 45 | 3650.4 | 2930.85 | 55.16 | 4133.6 | 3060 | 115.5 | 4398.4 | 3190.95 |
| 7 | 0 | 0 | 93.33 | 1,206.4 | 1,365.3 | 110.24 | 2,027.2 | 1,759.95 | 193.54 | 2,461.6 | 2,291.85 |
| 8 | 0 | 1.414 | 115 | 1,235.2 | 1,366.2 | 187.4 | 2,133.6 | 1,924.65 | 373.13 | 2,497.6 | 2,295 |
| 9 | 1.414 | 0 | 120 | 1,280 | 1,350 | 198.9 | 1,920 | 1,665 | 380 | 2,304 | 2,205 |
| 10 | 1 | 1 | 134.16 | 1,235.2 | 1,310.85 | 200.64 | 1,833.6 | 1,697.4 | 396.73 | 2,320 | 2,070 |
| 11 | 0 | 0 | 93.33 | 1,206.4 | 1,365.3 | 110.24 | 2,027.2 | 1,759.95 | 193.54 | 2,461.6 | 2,291.85 |
| 12 | 0 | –1.414 | 27 | 1,200 | 1,332 | 46.79 | 2,068.8 | 1,846.8 | 100 | 2,480 | 2,271.85 |
| 13 | –1 | –1 | 56.76 | 2,372.8 | 2,621.25 | 65.9 | 3,360 | 2,765.25 | 132 | 3,485.6 | 2,918.25 |

Table 5
ANOVA for the three models, PF, COD, TSS of UF20, UF50 and UF100

| Model | Response | Sum of squares | Degree of freedom | Mean square | *F*-value | *P*-value | $R^2$ |
|---|---|---|---|---|---|---|---|
| | PF | 10,503.26 | 5 | 2,100.65 | 29.87 | 0.0001 | 0.9536 |
| UF20 | COD | 6.716E+06 | 5 | 1.343E+06 | 65.62 | <0.0001 | 0.9712 |
| | TSS | 4.534E+06 | 5 | 9.068E+05 | 40.59 | <0.0001 | 0.9683 |
| | PF | 30,200.19 | 3 | 10,066.73 | 57.67 | <0.0001 | 0.9581 |
| UF50 | COD | 6.569E+06 | 5 | 1.314E+06 | 2,925.36 | <0.0001 | 0.9994 |
| | TSS | 3.180E+07 | 5 | 6.360E+06 | 93.32 | <0.0001 | 0.9852 |
| | PF | 1.138E+05 | 3 | 37,934.52 | 38.37 | <0.0001 | 0.9016 |
| UF100 | COD | 5.013E+06 | 5 | 1.003E+06 | 196.48 | <0.0001 | 0.9920 |
| | TSS | 1.510E+06 | 5 | 3.019E+05 | 152.23 | <0.0001 | 0.9987 |

$$Y_3 = +5{,}122.73799 - 1{,}067.01142X_1 - 68.2140X_2 - 5.58892X_1X_2 - 74.78134X_1^2 + 17.3755X_2^2 \quad (10)$$

$$Y_3 = +6{,}476.93696 - 688.18654X_1 - 2{,}618.11314X_2 - 6.29738X_1X_2 + 53.64867X_1^2 + 410.61963X_2^2 \quad (11)$$

$$Y_3 = +4{,}212.12376 - 538.82606X_1 + 5.80980X_2 + 1.8892X_1X_2 + 33.64223X_1^2 - 1.80000X_2^2 \quad (12)$$

Figs. 3–5 compare the experimental PF, COD and TSS values with the predicted data calculated by applying the regression equations [Eqs. (7)–(12)] for the three membranes. These graphics reveal that the model-predicted values are in accordance with the experimental values for the range studied. The coefficient of correlation is determined by the *R*-value. In Table 5 it can be seen that for all the membranes, the *R*-value is closer to unity, which demonstrates a positive relationship between the data.

### 3.3. Analysis of the effects of operating variables on permeate flux

Figs. 6–8 show the response surface graphs effect of TMP and CV on PF, COD and TSS respectively. The 3D response surface allows the interaction of these parameters to be visualized.

The ANOVA results indicate a significant effect of TMP and CV on PF for all three membranes. On the other hand, for DOC and TSS a significant effect of TMP is observed, however the effect of CV is found to be non-significant for all three membranes.

Fig. 6 shows the three-dimensional response surfaces for the interaction of TMP and CV on PF for the three membranes, a significant increase in TMP leads to an increase in PF based on Darcy's law [31,32]. The effects of CV on permeate flux are also significant in the range of 1.5–5 m/s, that is, the optimal CV values obtained for the maximum PF

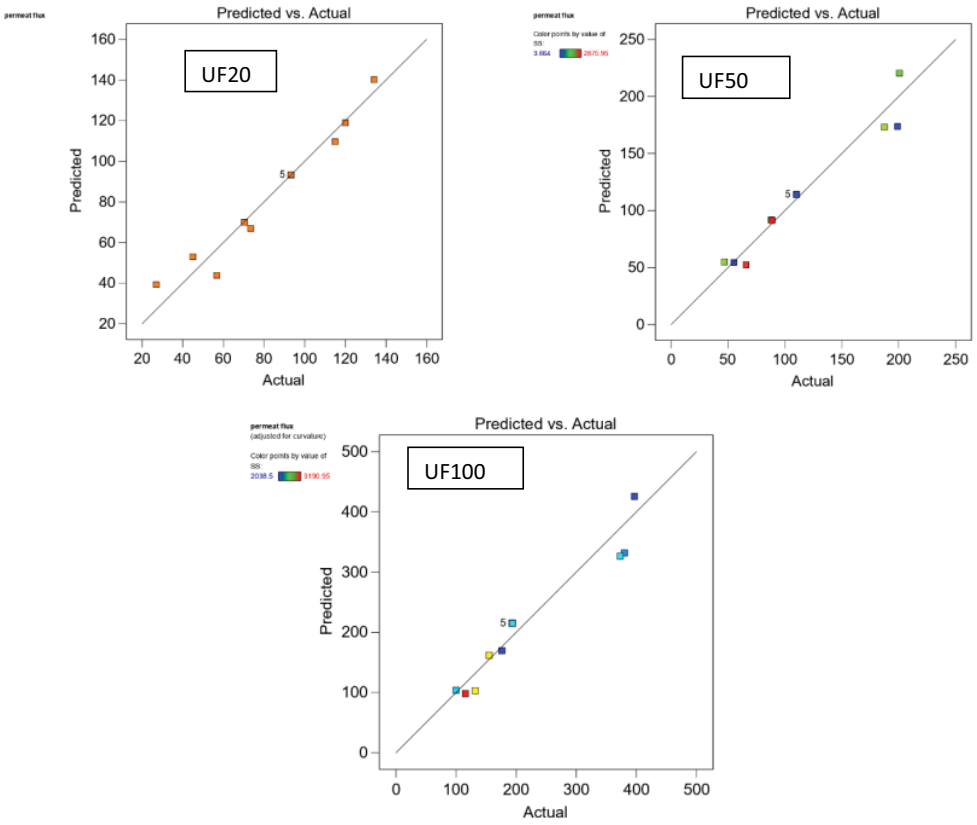


Fig. 3. Experimental and predicted PF values.

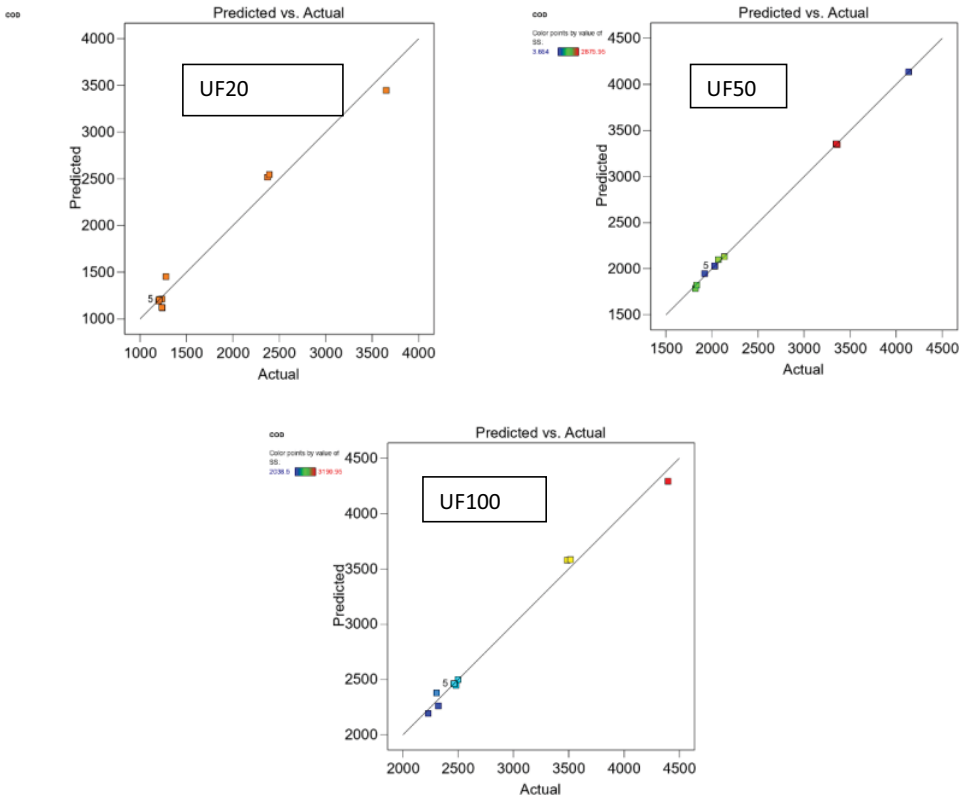


Fig. 4. Experimental and predicted values of COD.

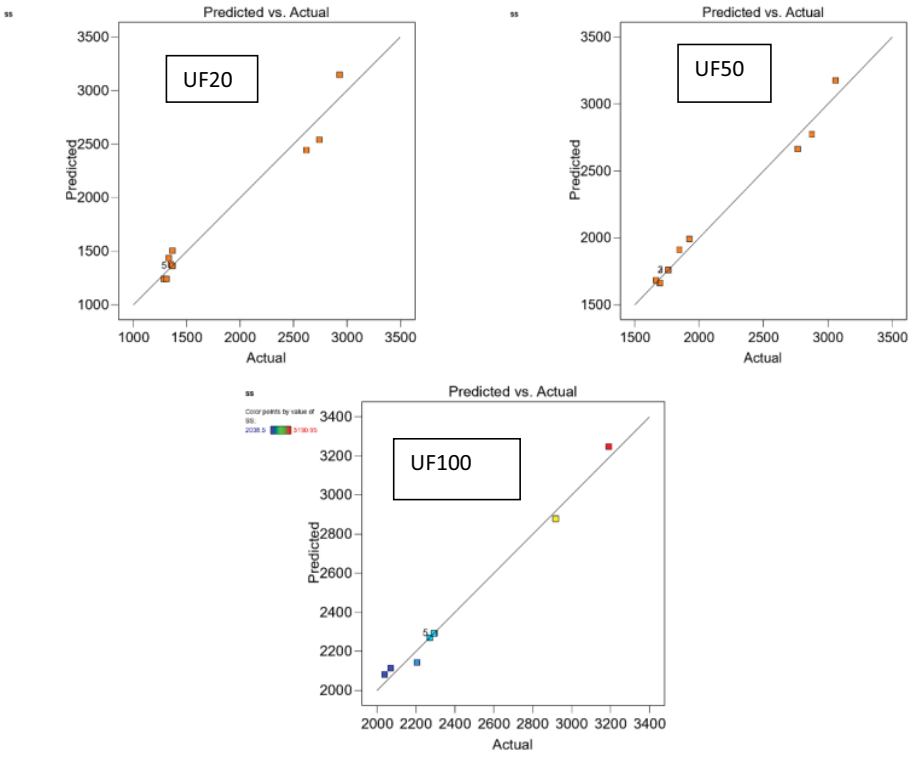


Fig. 5. Experimental and predicted values of TSS.

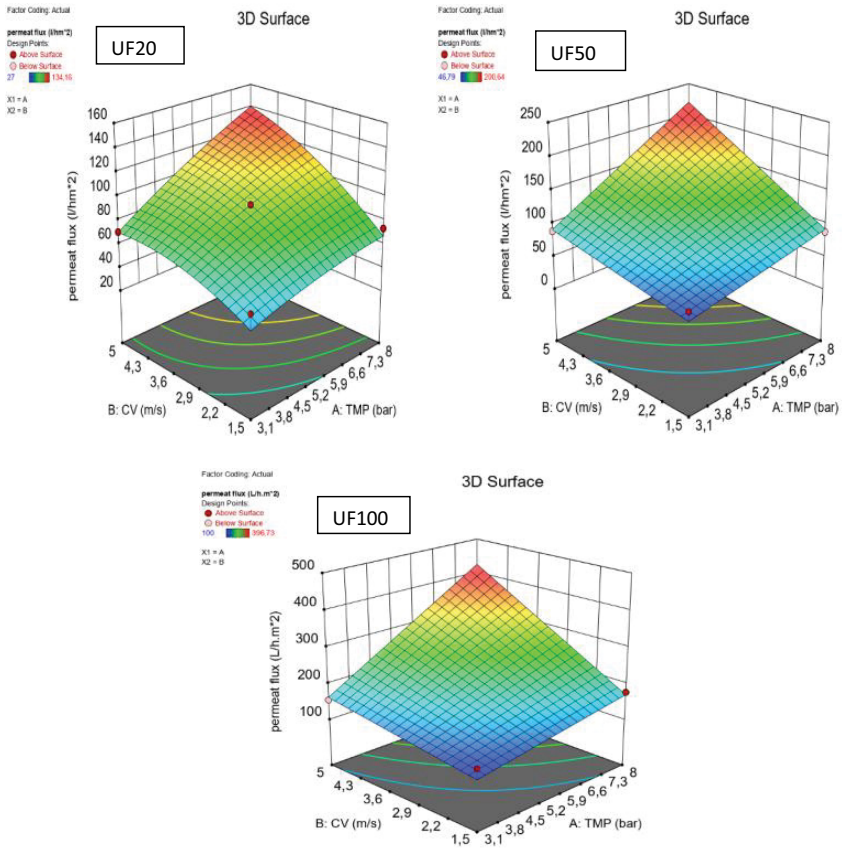


Fig. 6. Three-dimensional response surface curves of PF.

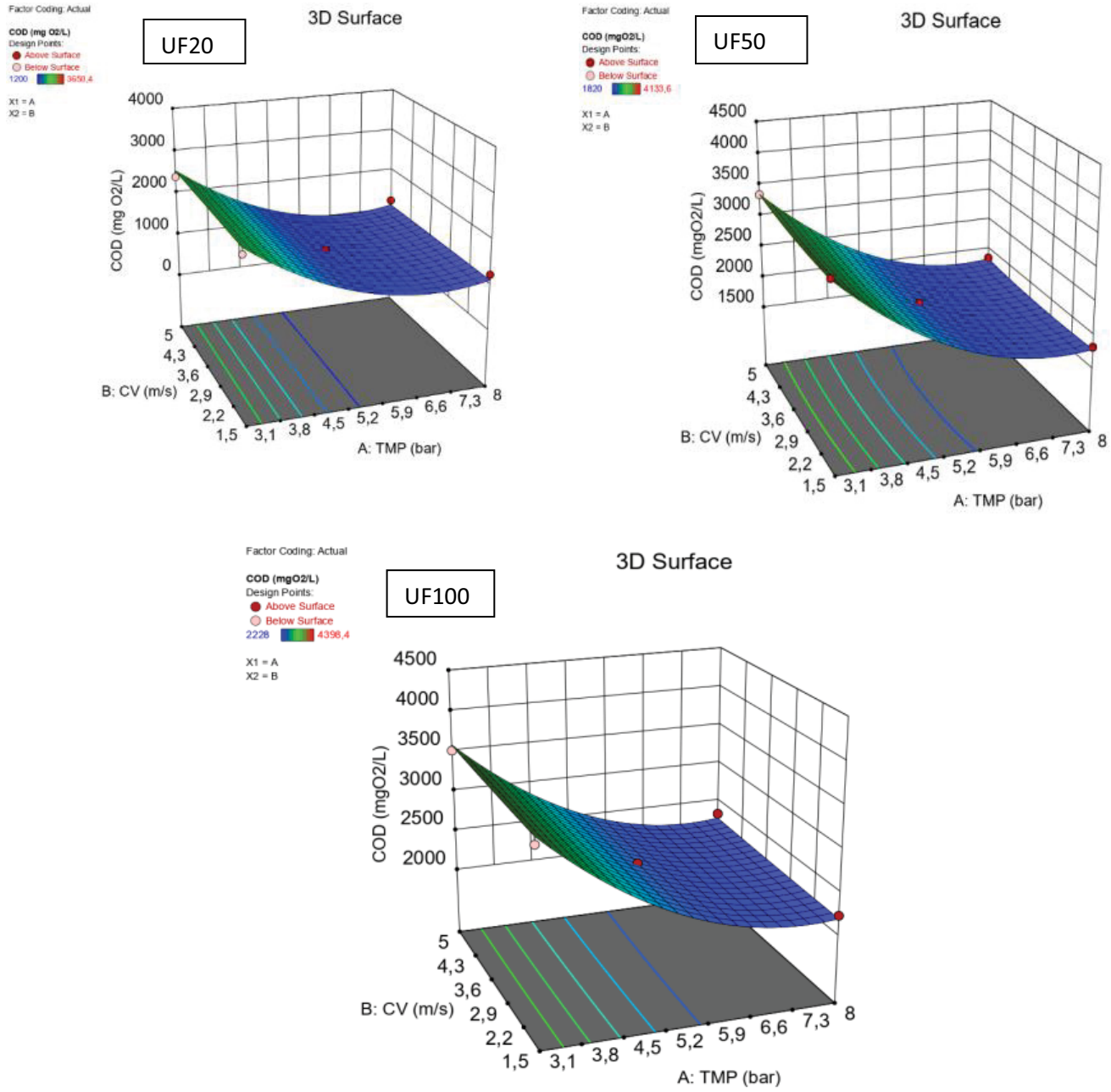


Fig. 7. Three-dimensional response surface curves of COD.

are (2.391, 2.793 and 2.798 m/s) for UF20, UF50, and UF100 respectively. According to the film model, the increase in velocity promotes turbulence, and thus can reduce the aggregation of LFL concentration in the membrane layer, therefore, it weakens the effect of concentration polarization and increases the PF [33]. On the other hand, the PF of UF100 nm is much higher than that of UF50 nm and UF20 nm. This is due to the pore size of the membranes which limits the permeate flux [34,35].

The interaction between TMP and CV on COD and TSS is illustrated in the three-dimensional response surface curves in Figs. 7 and 8 for UF20, UF50 and UF100. The efficiency of COD removal increases progressively in the higher ranges and stabilizes in the lower ranges at a TMP that does not exceed 5.9 bar for the three membranes. On the other hand, the efficiency of TSS removal increases with TMP and then reaches a plateau. For the UF20 membrane, the plateau starts at 5.5 bar and the TSS concentration drops to 1,364 mg/L, which corresponds to a rejection of 70%. Furthermore, UF50 and UF100 membranes, the plateau starts from 6 bar and the TSS rejection achieved is 62% for the UF50 and 50% for the UF100. Regardless CV value, the TSS content decreases with TMP ranging from 3 to 8 bar for all membranes.

As the TMP increases, more pollutants accumulate on the membrane surface, forming a gel layer and clogging the pores, leading to increased resistance to transfer and

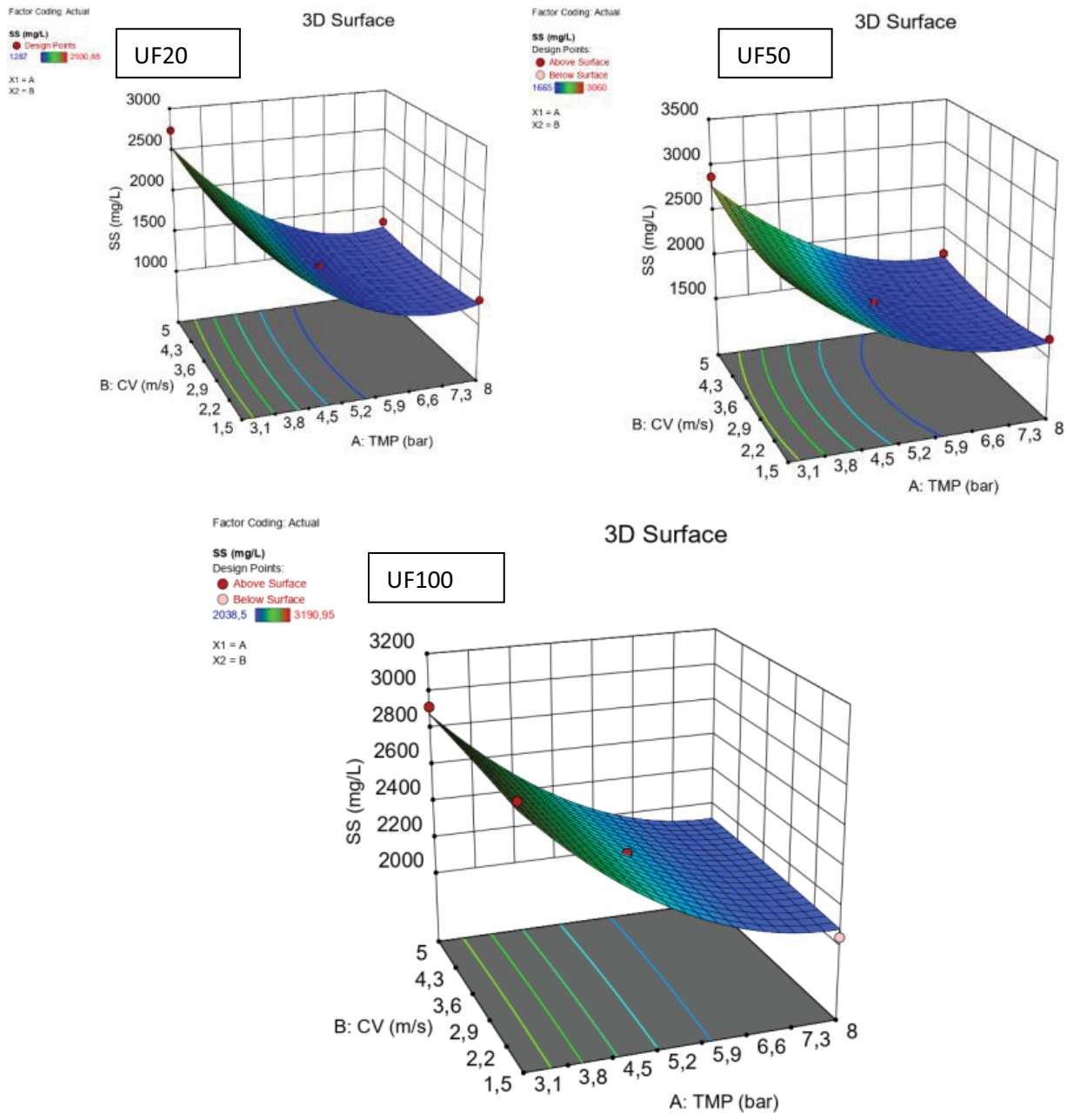


Fig. 8. Three-dimensional response surface curves of TSS.

the occurrence of limit flux due to the higher compression of pollutants. According to the gel polarization model, the existence of limit flux is related to the concentration polarization that occurs when the feed solution containing suspended and soluble solids (colloids). The accumulation of these colloids forms a viscous and gelatinous layer responsible for additional resistance to permeate flow in addition to that of the membrane [36], which explains the increase in pollutant retention and the formation of a plateau. Increasing CV has proven to be a suitable solution in order to reduce the concentration polarization phenomenon. Fig. 6 shows that CV has a significant effect on the PF, this effect is shown by the increase of the permeate limit flux across the three UF membranes with the increase of CV. According to the film model, an increase in CV improves the hydrodynamic conditions by reducing the concentration polarization layer, thus avoiding the formation of the fouling layer and improving the mass transfer coefficient, which leads to an increase in permeate flux [33].

However, according to Figs. 7 and 8, CV has no significant effect on COD and TSS removal, for an applied TMP. Indeed, the rejection of COD and TSS by the three membranes remains stable regardless the variation of CV. Then CV has no influence on the permeate quality. Thus, for the UF20 and for a TMP of 5.2 bar, the variation of the CV does not affect the rejection values of COD and TSS which remain

Table 6
Predicted responses by RSM and experimental data

| | UF20 | | UF50 | | UF100 | |
|---|---|---|---|---|---|---|
| TMP (bar) | 5.557 | | 5.970 | | 6.001 | |
| CV (m/s) | 2.391 | | 2.793 | | 2.798 | |
| | RSM | Exp. | RSM | Exp. | RSM | Exp. |
| PF (L/h m$^2$) | 78.908 | 74.64 | 105.846 | 110.25 | 207.761 | 198.21 |
| COD (mg $O_2$/L) | 1,200.015 | 1,184 | 1,907.839 | 2,027.2 | 2,345.607 | 2,461.6 |
| TSS (mg/L) | 1,364 | 1,360.35 | 1,678.667 | 1,858.5 | 2,223.376 | 2,291.8 |
| Desirability | 0.708 | – | 0.700 | – | 0.906 | – |

stables, 85% and 70.4% respectively. The same behavior is observed with the membranes UF50 and UF100.

## 4. Optimization of enhanced UF process

Table 6 gives the optimal conditions for the three UF membranes UF20, UF50 and UF100 using the desirability function approach, and the data found experimentally at the optimal conditions. Based on these results, a good agreement between the experimental and the theoretical conditions is obtained.

The economic operation of UF membrane process draws attention to the possibility of reducing costs in practice as for all processes. UF is cost effective with lower applied TMP (minimizing applied pressure) and lower CV (minimizing circulation velocity) to treat large volumes of LFL (maximizing permeate flux), as well as to achieve maximum rejection of COD and TSS.

## 5. Conclusion

The aim of this work is to study the feasibility of UF membranes in the reduction of pollution indicators of Oum Azza LFL with the ultimate goal of introducing UF separation in the existing processing chain upstream of RO. This study shows that, increasing the applied TMP for the three membranes causes a rise in PF until a limiting flux and improve the rejection of COD and TSS, Moreover, the CV has no influence on the rejection of COD and TSS. On the other hand, PF fluxes and limiting fluxes have been improved with the increase of the CV.

Furthermore, RSM is one of the appropriate methods to optimize the operating conditions minimizing the TMP and CV and maximizing the COD and TSS rejection and PF for UF20, UF50 and UF100. The analysis of variance shows a high value of the coefficient of determination ($R^2 > 0.90$), thus ensuring a satisfactory fit of the second-order regression model with the experimental data. The optimization of the models results in the following conclusions:

- TMP and CV have a significant effect of on PF for the three membranes.
- The effects of CV on PF are also significant in the range of 1.5–5 m/s, with an optimal values 2.391, 2.793 and 2.798 m/s for UF20, UF50, and UF100 respectively.
- TMP has a significant effect on the retention of COD and TSS. However, CV has no influence on the rejection of COD and TSS and consequently on the quality of the permeate.

## Acknowledgement

This work was supported by the Delegate Ministry in charge of the Environment in Morocco. The authors express their thanks for this support.

## References

[1] V. Vatanpour, S.S. Madaeni, A.R. Khataee, E. Salehi, S. Zinadini, H.A. Monfared, $TiO_2$ embedded mixed matrix PES nanocomposite membranes: influence of different sizes and types of nanoparticles on antifouling and performance, Desalination, 292 (2012) 19–29.
[2] A. Mousavinejad, A. Rahimpour, M.R. Shirzad Kebria, S. Khoshhal Salestan, M. Sadrzadeh, N.V.H. Kiadeh, Nickel-based metal–organic frameworks to improve the $CO_2/CH_4$ separation capability of thin-film pebax membranes, Ind. Eng. Chem. Res., 59 (2020) 12834–12844.
[3] L. Zhang, A. Li, Y. Lu, L. Yan, S. Zhong, C. Deng, Characterization and removal of dissolved organic matter (DOM) from landfill leachate rejected by nanofiltration, Waste Manage., 29 (2009) 1035–1040.
[4] Y. Deng, J.D. Englehardt, Treatment of landfill leachate by the Fenton process, Water Res., 40 (2006) 3683–3694.
[5] A.H. Robinson, Landfill leachate treatment, Membr. Technol., 2005 (2005) 6–12.
[6] E. Hassanzadeh, M. Farhadian, A. Razmjou, N. Askari, An efficient wastewater treatment approach for a real woolen textile industry using a chemical assisted NF membrane process, Environ. Nanotechnol. Monit. Manage., 8 (2017) 92–96.
[7] P.J. Kaur, U. Chandra, C.M. Hussain, G. Kaushik, Chapter 13 – Landfarming: A Green Remediation Technique, in: The Handbook of Environmental Remediation: Classic and Modern Techniques, Royal Society of Chemistry, United Kingdom, 2020, pp. 357–378.
[8] A. Kallel, M. Ellouze, I. Trabelsi, Co-management of landfill leachate concentrate with brick waste by solidification/stabilization treatment, Arabian J. Geosci., 10 (2017) 81, doi: 10.1007/s12517-017-2871-x.
[9] R. He, B.-H. Tian, Q.-Q. Zhang, H.-T. Zhang, Effect of Fenton oxidation on biodegradability, biotoxicity and dissolved organic matter distribution of concentrated landfill leachate derived from a membrane process, Waste Manage., 38 (2015) 232–239.
[10] J. Xu, Y. Long, D. Shen, H. Feng, T. Chen, Optimization of Fenton treatment process for degradation of refractory organics in pre-coagulated leachate membrane concentrates, J. Hazard. Mater., 323 (2017) 674–680.
[11] H.-w. Wang, X.-y. Li, Z.-p. Hao, Y.-j. Sun, Y.-n. Wang, W.-h. Li, Y.F. Tsang, Transformation of dissolved organic matter in concentrated leachate from nanofiltration during

ozone-based oxidation processes ($O_3$, $O_3/H_2O_2$ and $O_3$/UV), J. Environ. Manage., 191 (2017) 244–251.
[12] I.A. Tałałaj, P. Biedka, I. Bartkowska, Treatment of landfill leachates with biological pretreatments and reverse osmosis, Environ. Chem. Lett., 17 (2019) 1177–1193.
[13] C. Chiemchaisri, W. Chiemchaisri, P. Nindee, C.Y. Chang, K. Yamamoto, Treatment performance and microbial characteristics in two-stage membrane bioreactor applied to partially stabilized leachate, Water Sci. Technol., 64 (2011) 1064–1072.
[14] J. Liu, H. Zhang, P. Zhang, Y. Wu, X. Gou, Y. Song, Z. Tian, G. Zeng, Two-stage anoxic/oxic combined membrane bioreactor system for landfill leachate treatment: pollutant removal performances and microbial community, Bioresour. Technol., 243 (2017) 738–746.
[15] N. Elfilali, N. Essafi, M. Zait, M. Tahaikt, F. Elazhar, A. Elmidaoui, M. Taky, Effectiveness of membrane bioreactor/reverse osmosis hybrid process for advanced purification of landfill leachate, Desal. Water Treat., 240 (2021) 24–32.
[16] M.C.S. Amaral, W.G. Moravia, L.C. Lange, M.M.Z. Roberto, N.C. Magalhães, T.L. dos Santos, Nanofiltration as post-treatment of MBR treating landfill leachate, Desal. Water Treat., 53 (2015) 1482–1491.
[17] Z. Li, S. Zhou, J. Qiu, Combined treatment of landfill leachate by biological and membrane filtration technology, Environ. Eng. Sci., 24 (2007) 1245–1256.
[18] M. Zait, S. Benalla, B. Bachiri, M. Tahaikt, D. Dhiba, A. Elmidaoui, M. Taky, Performance of three ultrafiltration ceramic membranes in reducing polluting load of landfill leachate, Desal. Water Treat., 240 (2021) 33–42.
[19] M.A. Bezerra, R.E. Santelli, E.P. Oliveira, L.S. Villar, L.A. Escaleira, Response surface methodology (RSM) as a tool for optimization in analytical chemistry, Talanta, 76 (2008) 965–977.
[20] S. Popovic, M. Karadžic, J. Cakl, Optimization of ultrafiltration of cutting oil wastewater enhanced by application of twisted tapes: response surface methodology approach. J. Cleaner Prod., 231 (2019) 320–330.
[21] L.M. Collins, S.A. Murphy, V.N. Nair, V.J. Strecher, A strategy for optimizing and evaluating behavioral interventions, Ann. Behav. Med., 30 (2005) 65–73.
[22] M. Zolfaghari, K. Jardak, P. Drogui, S.K. Brar, G. Buelna, R. Dubé, Landfill leachate treatment by sequential membrane bioreactor and electro-oxidation processes, J. Environ. Manage., 184 (2016) 318–326.
[23] C. Cojocaru, G. Zakrzewska-Trznadel, Response surface modeling and optimization of copper removal from aqua solutions using polymer assisted ultrafiltration, J. Membr. Sci., 298 (2007) 56–70.
[24] M.C.M. Calatayud, M.C.V. Vela, S.Á. Blanco, J.L. García, E.B. Rodríguez, Analysis and optimization of the influence of operating conditions in the ultrafiltration of macromolecules using a response surface methodological approach, J. Chem. Eng., 156 (2010) 337–346.
[25] M. Darvishmotevalli, A. Zarei, M. Moradnia, M. Noorisepehr, H. Mohammadi, Optimization of saline wastewater treatment using electrochemical oxidation process: prediction by RSM method. MethodsX, 6 (2019) 1101–1113.
[26] S.M.A. Abuabdou, B.J.K. Mohammed, N. Choon Aun, S. Sumathi, Y. Wong Ling, Development of a novel polyvinylidene fluoride membrane integrated with palm oil fuel ash for stabilized landfill leachate treatment, J. Cleaner Prod., 311 (2021) 127677, doi: 10.1016/j.jclepro.2021.127677.
[27] B.J.K. Mohammed, A.A. Hamidi, A.A.S. Salem, S. Sumathi a/p, N. Choon Aun, L. Jun Wei, The competency of various applied strategies in treating tropical municipal landfill leachate, Desal. Water Treat., 54 (2015) 2382–2395.
[28] S.M.A. Abuabdou, W. Ahmad, N. Choon Aun, B.J.K. Mohammed, A review of anaerobic membrane bioreactors (AnMBR) for the treatment of highly contaminated landfill leachate and biogas production: effectiveness, limitations and future perspectives, J. Cleaner Prod., 255 (2020) 120215, doi: 10.1016/j.jclepro.2020.120215.
[29] Preservation of the Quality of Water Resources and Fight Against Pollution, Ministry Delegated to the Minister of Energy, Mines, Water and the Environment, Loaded with Water, Direction of the Research and Planning the Water, Water Quality Division, Water Pollution Control Service, Morocco, June 2014.
[30] Y. Zheng, A. Wang, Removal of heavy metals using polyvinyl alcohol semi-IPN poly(acrylic acid)/tourmaline composite optimized with response surface methodology, Chem. Eng. J., 162 (2010) 186–193.
[31] F.L. Hua, Y.F. Tsang, Y.J. Wang, S.Y. Chan, H. Chua, S.N. Sin, Performance study of ceramic microfiltration membrane for oily wastewater treatment, J. Chem. Eng., 128 (2007) 169–175.
[32] A.L. Ahmad, S. Ismail, S. Bhatia, Ultrafiltration behavior in the treatment of agro-industry effluent: pilot scale studies, Chem. Eng. Sci., 60 (2005) 5385–5394.
[33] J.L. Nilsson, Protein fouling of UF membranes: causes and consequence, J. Membr. Sci., 52 (1990) 121–142.
[34] S. Bunani, E. Yorükoglu, G. Sert, Ü. Yüksel, M. Yüksel, N. Kabay, Application of nanofiltration for reuse of municipal wastewater and quality analysis of product water, Desalination, 315 (2013) 33–36.
[35] S. Shanmuganathan, S. Vigneswaran, T.V. Nguyen, P. Loganathan, J. Kandasamy, Use of nanofiltration and reverse osmosis in reclaiming micro-filtered biologically treated sewage effluent for irrigation, Desalination, 364 (2015) 119–125.
[36] S. Qaid, M. Zait, K. El Kacemi, A. El Midaoui, H. El Hajji, M. Taky, Ultrafiltration for clarification of Valencia orange juice: comparison of two flat sheet membranes on quality of juice production, J. Mater. Environ. Sci., 8 (2017) 1186–1194.